ISSN 2063-5346

EARLY PREDICTION AND CLASSIFICATION OF LUNG CANCER THROUGH THE MEASUREMENT OF EFFECTIVE PARAMETERS USING CT IMAGES

Dr.G.R.JothiLakshmi[1*], G.Shreyahs[2], R.Jaheen Sha[3]

[1]Associate professor, [2,3] UG Scholars,

Department of Electronics and Communication Engineering, Vels Institute of Science,Technology& Advanced Studies(VISTAS),Chennai-600117, Tamilnadu, India

*Corresponding Author: jothi.se@velsuniv.ac.in

Article History: Received: 03.04.2023 **Revised:** 25.04.2023 **Accepted:** 15.05.2023

Abstract

Cellular breakdown in the lungs is one of the most compromising sicknesses among any remaining lung problems which is caused for uncontrolled cell development. The discovery of cellular breakdown in the lungs in beginning phases is the vitally understandable way to deal with upgrade patient's endurance rate. Picture Handling along with profound growing experience and different advances are utilized to read up clinical pictures for prior recognition. A considerable lot of explores have been made for cellular breakdown in the lungs recognition utilizing Processed Tomography (CT) pictures. This examination incorporates reflection coefficient with CNN calculation of lung cancerdetection that shows better results.The exactness pace of the many papers is around 98.22% is accomplished by their methods.We were utilized various advances like improvement utilizing medianfilter, division, highlight extraction and Grouping utilizing CNN. The removed elements are contrast, relationship, energy, mean, Standard Deviation, fluctuation, reflection coefficient, kurtosis, skewness.Finally, the analysis result showsthe characterization exactness execution of 99.2%.

Keywords: *Lung Cancer, CT Scan Images, Computer-Aided Diagnosis, CNN, Feature Extraction*.

I. INTRODUCTION

The cellular breakdown in the lungs is one of risky disease, it is situated in lung. Malignant growth is made of unusual cell that develops even the body doesn't need, disease begins when cells are outgrows control. This strange cells in the body develop to type of mass or light called growth and assuming these phones are in the body for long time they can fill in to local regions.

II. RELATED WORKS

Large numbers of investigates have been made for lung cancer detection utilizing Registered Tomography (CT) pictures. This exploration is all connected with our proposedmethod. This exploration incorporates reflection coefficient with CNN calculation of lung cancerdetection that shows better results.The precision pace of the many papers is around 98.22% is accomplished by their techniques

III. PROPOSED SYSTEM

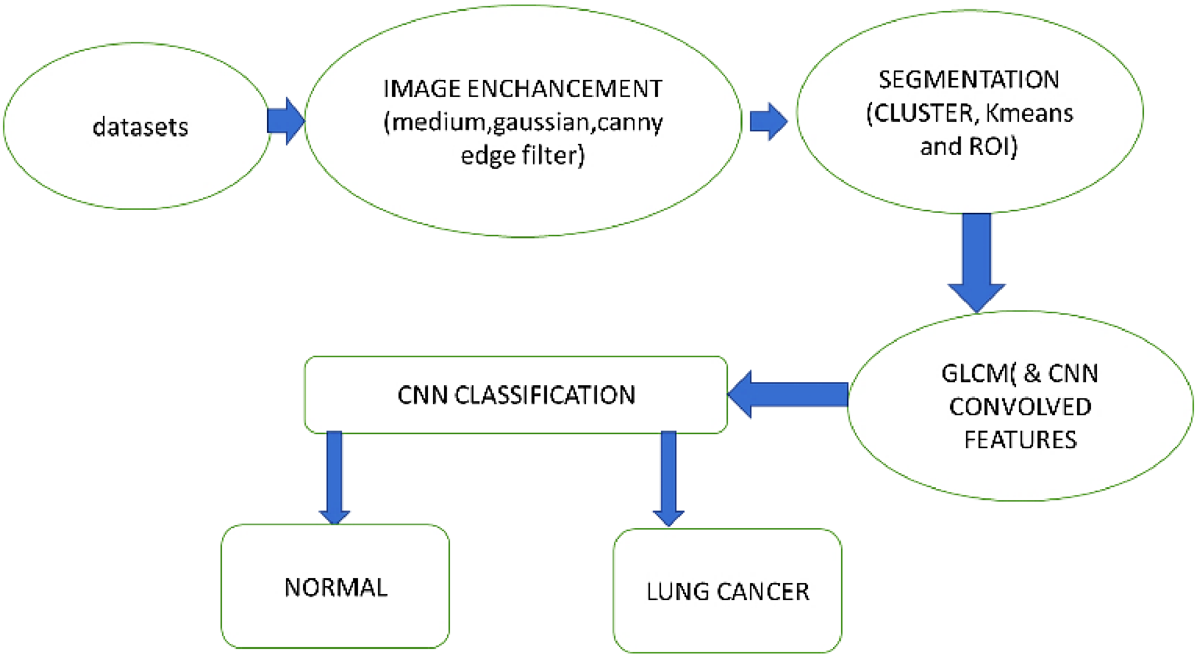

A. Median filter

Medium filtration is a roundabout method for lessening fast commotion, likewise called salt and pepper clamor. It can likewise be utilized to safeguard the edges of a picture while limiting irregular sound. The middle channel for the ongoing pixel region is 10, which is a medianof five values.The focal channel checks every pixel in the picture and contrasts it and its neighbors to decide whether it addresses the encompassing region. Rather than just setting the pixel esteem and the importance of the closest pixel esteems, the middle of those values is utilized all things being equal. Media is determined by arranging all the pixel values in the encompassing region by mathematical request, and afterward rotating the pixel being referred to into the media.

B. K-means clustering

Information mining typically uses K-implies grouping, a vector quantization technique derived from signal handling, for bunch investigation. The goal of K-implies bunching is to divide n perceptions into k groups so that each perception may be found in the group with the closest mean, which serves as the bunch model. The information space is divided into Voronoi cells as is appropriate.Computingly challenging problem (NP-hard); nonetheless, there are efficient heuristic calculations that are frequently used and that quickly connect to a neighbourhood ideal. Through the iterative screening method used in both calculations, they are frequently similar to the assumption boost calculation for a mixture of Gaussian dispersions. Additionally, both employ group communities for information display. However, k-implies bunching will often look for groups with a similar spatial degree, but the assumption expansion component allows for groups of different forms.

The calculation has a free relationship with the k-closest neighbour classifier, a well-known order-determining AI technique that, because to the k in its name, is sometimes confused with k-implies. To organise new information in existing bunches, closest neighbour classifier can be applied to group locations gathered by k-means. This is sometimes referred to as Rocchio's computation or the closest centroid classifier.

C. Canny edge filter

A multi-stage algorithm is used by the Shrewd edge identifier, an edge discovery administrator, to identify numerous edges in photos.The bustle in the image is less noticeable because to the Gaussian. Then, by removing non-most extreme pixels of the angle magnitude, possible edges are weakened to 1-pixel bends.The Vigilant method locates edges by looking for neighbourhood maxima of the image's inclination.The fact that Watchful is able to distinguish much more edges than Sobel does suggests that Shrewd's edge finder performs better than Sobel's edge locator.

D. Pattern recognition

Designing is an interaction that involves taking things out of a given picture and changing how we see those things. The RF handling technique and the picture handling approach are the two standard approaches to handling the issue of example acknowledgment. Electromagnetic waves are transmitted and then reflected from the target in the RF handling method. To determine the objective, the reflected waves are examined.When the target is very far away or out of sight, the RF handling is typically used. An image or picture of the field is taken in the picture handling approach. Then, to see the items in the image, the image is handled and studied.

Reflection Coefficient

The abundance of the reflected wave relative to the incident wave determines the reflection coefficient. It shows the volume of waves that can be reflected from a material or medium's surface. It is used in optics to determine how much light a holder's outer layer reflects.

Ruggedness to shifts and distortion in the image

CNN locations are difficult to manipulate, such as changing shape due to camera focus, variable lighting conditions, different positions, the presence of midway obstructions, level and vertical movements, and so forth. Despite this, CNNs are shift invariant since they use the same weight arrangement everywhere. Theoretically, we can also get shift invariants by using totally associated layers. . However, the outcome of anticipating this scenario is a variety of units with identical weight designs scattered throughout the information. The space of conceivable variants would need to be covered by a staggering number of preparation events in order to become comfortable with these weight designs.

Feature Extraction

In picture handling, highlight extraction begins from an underlying arrangement of estimated information and fabricates determined values (highlights) planned to be educational and non-excess, working with the resulting learning and speculation steps, and now and again prompting better human understandings. Highlight extraction is connected with dimensionality decrease.

At the point when the information to a calculation is too enormous to possibly be handled and it is thought to be excess (e.g., similar estimation in the two feet and meters, or the monotony of pictures introduced as pixels), then, at that point, it tends to be changed into a diminished arrangement of elements (likewise named a highlights vector). This cycle is called include choice. The chose highlights are supposed to contain the significant data from the information, with the goal that the ideal undertaking can be performed by utilizing this diminished portrayal rather than the total starting information.

Step1. Read image.
Step2. .Picture resize to all picture in data set.
Step3. Decay variety picture utilizing Haar DWT at first level to getapproximatecoefficient and culpa detail coefficients.

Step4. Allot the loads 0.003 to surmised coefficients.
Step5. Convert the rough coefficient picture in to HSV plane.
Step6. Variety quantization is completed utilizing variety histogram by doling out 18 canisters to tint, and 3 containers to immersion and 4 receptacles to worth to give a quantized HSV space with 18+3+4=25 histogram containers.
Step7. Rehash step1 to step6 on a picture in the data set.
Step8. Compute the similitude network of question picture and the picture present in the data set.
Step9. Rehash the means from 7 to 8 for every one of the pictures in the data set.
Step10. Recover the pictures.

Result
Abnormal Image Value

S.no	Input image	Contrast	Correlation	Energy	Mean	Standard Deviation	Variance	Reflection coefficient	Skewness	Kurtosis	numFm	Dropout	Size Fm	Size out	numFm	Dropout	Size out	numFm	Dropout	numweight	Num Fm	Size Fm	Size Output
											Layer 1 input		Layer 2 fc		Layer 3 fc2			Layer 4 softmax			Layer 5 output		
1.	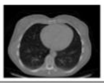	0.2931	0.1490	0.7804	0.0057	0.0896	0.0081	0.9552	1.2404	14.8773	1	1	1	1 128	16	1	1 16	16	1	0	16	1	1 16
2.	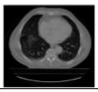	0.2681	0.1309	0.7733	0.0043	0.0897	0.0080	0.9418	0.8117	10.4398	1	1	1	1 126	16	1	1 16	16	1	0	16	1	1 16
3.		0.2681	0.1309	0.7738	0.0029	0.0898	0.0081	0.9144	0.7682	9.9853	1	1	1	1 128	16	1	1 16	16	1	0	16	1	1 16
4.	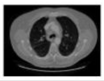	0.2792	0.0881	0.7614	0.0040	0.0897	0.0080	0.9370	0.8508	10.1824	1	1	1	1 128	16	1	1 16	16	1	0	16	1	1 16
5.		0.2425	0.1171	0.7739	0.0031	0.0898	0.0080	0.9210	0.5087	7.9308	1	1	1	1 126	16	1	1 16	16	1	0	16	1	1 16
6.		0.2597	0.1286	0.7740	0.0039	0.0897	0.0081	0.9361	0.9398	0.6021	1	1	1	1 128	16	1	1 16	16	1	0	16	1	1 16
7.		0.2870	0.0522	0.7637	0.0026	0.0898	0.0080	0.9056	0.9848	12.2682	1	1	1	1 126	16	1	1 16	16	1	0	16	1	1 16
8.	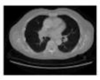	0.2278	0.1203	0.7473	0.0039	0.0897	0.0080	0.9348	0.4410	6.3497	1	1	1	1 128	16	1	1 16	16	1	0	16	1	1 16

9.		0.2665	0.1447	0.7630	0.0052	0.0897	0.0081	0.9557	0.9752	12.5761	1	1	1	1 126	16	1	1 16	16	1	0	16	1	1 16
10.		0.2681	0.1309	0.7733	0.0043	0.0897	0.0080	0.9418	0.8117	10.4398	1	1	1	1 128	16	1	1 16	16	1	0	16	1	1 16
11.		0.2870	0.0522	0.7637	0.0046	0.0882	0.0080	0.9856	0.9844	9.3542	1	1	1	1 128	16	1	1 16	16	1	0	16	1	1 16
12.		0.2739	0.0634	0.7689	0.0026	0.0898	0.0080	0.9056	0.9848	12.2682	1	1	1	1 126	16	1	1 16	16	1	0	16	1	1 16
13.		0.2635	0.1457	0.7730	0.0043	0.0897	0.0081	0.9557	0.9752	10.5478	1	1	1	1 128	16	1	1 16	16	1	0	16	1	1 16
14.	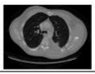	0.2635	0.0682	0.7264	0.0051	0.0897	0.0081	0.9557	0.9768	12.5528	1	1	1	1 128	16	1	1 16	16	1	0	16	1	1 16
15.		0.2567	0.0814	0.7637	0.0052	0.0897	0.0080	0.9776	0.9752	12.5761	1	1	1	1 126	16	1	1 16	16	1	0	16	1	1 16
16.		0.2681	0.1309	0.7733	0.0043	0.0897	0.0080	0.9210	0.5087	7.9308	1	1	1	1 128	16	1	1 16	16	1	0	16	1	1 16
17.		0.2681	0.1309	0.7630	0.0052	0.0897	0.0081	0.9210	0.5087	7.9308	1	1	1	1 126	16	1	1 16	16	1	0	16	1	1 16
18.		0.2870	0.0522	0.7689	0.0026	0.0898	0.0080	0.9418	0.8117	10.4398	1	1	1	1 126	16	1	1 16	16	1	0	16	1	1 16
19.		0.2931	0.1490	0.7804	0.0057	0.0896	0.0081	0.9552	1.2404	14.8773	1	1	1	1 128	16	1	1 16	16	1	0	16	1	1 16
20.		0.2635	0.1457	0.7730	0.0043	0.0897	0.0081	0.9557	0.9752	10.5478	1	1	1	1 126	16	1	1 16	16	1	0	16	1	1 16
AVARAGE		0.2656 875	0.11463 75	0.76847 5	0.0038	0.08972 5	0.00703 75	0.930737 5	0.81817 5	10.20445	1	1	1	1 127	16	1	1 16	16	1	0	16	1	1 16

Normal Values

S.no	Input image	Contrast	Correlation	Energy	Mean	Standard Deviation	Variance	Reflection coefficient	Skewness	Kurtosis	num Fm	Drop out	SizeFm	Size out	numFm	Dropout	Size out	num Fm	Drop out	num weight	Fr Fm	Fm	ut
											Layer 1 input		Layer 2 fc		Layer 3 fc2			Layer 4 softmax			Layer 5 output		
1.		0.2447	0.0923	0.7313	0.0037	0.0897	0.0080	0.9325	0.476	6.2138	1	1	1	1 128	16	1	1 16	16	1	0	16	1	1 16
2.		0.2447	0.0923	0.7313	0.0037	0.0897	0.0080	0.9325	0.476	6.2138	1	1	1	126	16	1	1 16	16	1	0	16	1	1 16
3.		0.2191	0.0971	0.7599	0.0025	0.0898	0.0081	0.9015	0.5448	5.9798	1	1	1	1 128	16	1	1 16	16	1	0	16	1	1 16
4.		0.2191	0.0971	0.7599	0.0025	0.0898	0.0081	0.9015	0.5448	5.9798	1	1	1	1 128	16	1	1 16	16	1	0	16	1	1 16
5.		0.2414	0.0588	0.7528	0.0013	0.0898	0.0081	0.8330	0.5573	6.4467	1	1	1	126	16	1	1 16	16	1	0	16	1	1 16
6.		0.2475	0.0954	0.7387	0.0033	0.0898	0.0080	0.9247	0.6642	6.5309	1	1	1	1 128	16	1	1 16	16	1	0	16	1	1 16
7.	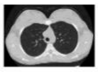	0.2358	0.1183	0.7520	0.0040	0.0897	0.0080	0.9365	0.5133	7.0753	1	1	1	126	16	1	1 16	16	1	0	16	1	1 16
8.	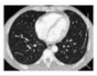	0.2297	0.1051	0.7449	0.0042	0.0897	0.0081	0.9396	0.5094	5.9154	1	1	1	1 128	16	1	1 16	16	1	0	16	1	1 16

Abnormal

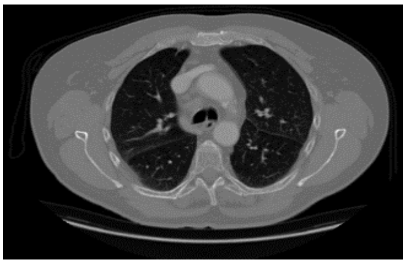

Normal

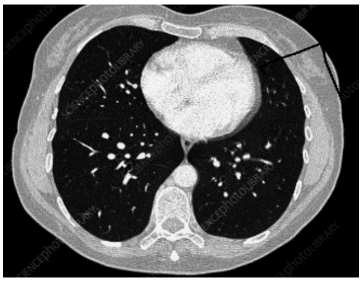

CONCLUSION

Cellular breakdown in the lungs is the most perilous and boundless on the planet as per stage the revelation of the malignant growth cells in the lungs. A picture improvement method assumes a vital and fundamental part to keep away from serious stages and to diminish its rate circulation in the world.Many of explores have been made for cellular breakdown in the lungs discovery utilizing Registered Tomography (CT) pictures. This examination is all connected with our proposed strategy. This examination incorporates reflection coefficient with CNN calculation of cellular breakdown in the lungs identification that shows improved results. The exactness pace of the many papers is around 98.22% is accomplished by their strategies.

REFERENCES

1. O. Abuzaghleh, B. D. Barkana, and M. Faezipour, “SKIN cure: A real time image analysis system to aid in the malignant skin cancer prevention and early detection”in Proc. IEEE Southwest Symp. Image Anal. Interpretation (SSIAI), Apr. 2014, pp.85_88.

2. M. Silveira, J. C. Nascimento, J. S. Marques, A. R. Marcal, T. Mendonca, S. Yamauchi, J. Maeda, and J. Rozeira, Comparison of segmentation methods for skin cancer diagnosis in dermoscopy images, "Selected Topics in Signal Processing, IEEE Journal of, vol. 3, no. 1, pp.35–45, 2009.
3. N. K. Mishra and M. E. Celebi, "An overview of skin cancer detection in dermoscopy images using image processing and machine learning," arXiv preprint arXiv:1601.07843, 2016.
4. N. Codella, J. Cai, M. Abedini, R. Garnavi, A. Halpern, and J. R. Smith, "Deep learning, sparse coding, and SVM for skin cancer recognition in dermoscopy images," in Machine Learning in Medical Imaging. Springer, 2015, pp. 118–126.
5. A. F. Jerant, J. T. Johnson, C. Sheridan, T. J. Caffrey et al., "Early detection and treatment of skin cancer," American family physician, Vol. 62, no. 2, pp. 357–386, 2000.
6. Patwardhan, S.V., Dhawan, A.P., Relue, P.A.: 'Classification of skin cancer using tree structured wavelet transforms', Compute Methods Programs Biomed., 2003,72, (3), pp. 223–239
7. Iyatomi. H., Oka, H., Celebi, M.E.: 'An improved internet-based skin cancer screening system with dermatologist-like tumor area extraction algorithm', Compute. Med. Imaging Graph, 2008, 32, (7), pp. 566–579
8. Commonly diagnosed cancer worldwide, Cancer research UK, April 2005.
9. WHO Disease and injury country estimates, World Health Organization, 2009.
10. Jemal, A., R.C. Tiwari, T. Murray, A. Ghafoor, A. Samuels, El. Ward, E.J. Feuer, and M.J. Thun, Cancer statistics, 2004. CA Cancer J Clin, 2004. 54(1): p.8-29.
11. Salomaa ER, Sällinen S, Hiekkanen H, Liippo K, "Delays in the diagnosis and treatment of lung cancer", Chest, 2005 Oct, 128(4):2282- 8.
12. Strauss, GM, Gleason, RE, Sugarbaker, "DJ Screening for lung cancer: another look; a different view", Chest 1997;111,754-768.
13. Toriwaki J.I., Suenaga Y., Negoro T., Fukumura T., "Pattern recognition of Chest X-ray Images", Computer Graphics and Image Processing, Vol. 2, Issue. 3-4, December 1973, pp. 252-271.
14. Patil, S.A. Udupi, V.R. Kane, C.D. Wasif, A.I. Desai, J.V. Jadhav, A.N., "Geometrical and Texture Features Estimation of Lung Cancer and TB Images Using Chest X-Ray Database", Biomedical and Pharmaceutical Engineering, 2009, ICBPE '09 International Conference, 2-4 Dec. 2009.
15. Xu X.W, Doi K., Kobayashi T., MacMahon H, Giger M.L., "Development of an Improved CAD Scheme for Automated Detection of Lung Nodules in Digital Chest Images", Medical Physics 24, 1395 (1997); doi:10.1118/1.598028.
16. Brown M.S., Goldin J.G, Suh R.D., McNitt-Gray M.F., Sayre J.W., Aberle D.R., "Lung Micronodules: Automated Method for Detection at Thin-Section CT Initial Experience", Radiology, 226, January 2003, pp. 256-262.
17. Farag A. A., El-Baz A., Gimelfarb G.G., Falk R., Hushek S.G., "Automatic Detection and Recognition of Lung Abnormalities in Helical CT Images Using Deformable Templates", Medical Image Computing and Computer-Assisted Intervention – MICCAI 2004.
18. Gurcan M.N., Sahiner B., Petrick N.,

Chan H.P., Kazerooni E.A., Cascade P.N., Hadjiiski L., "Lung Nodule Detection on Thoracic Computed Tomography Images: Preliminary Evaluation of a Computer Aided Diagnosis System", Medical Physics 29, 2552, 2002.

19. Brown, M.S., McNitt-Gray, M.F., Goldin, J.G., Suh, R.D., Sayre, J.W., Aberle, D.R, "Patient-Specific Models for Lung Nodule Detection and Surveillance in CT Images", IEEE Transactions on Medical Imaging, Dec. 2001, Vol. 20, Issue. 12, pp. 1242-1250.

20. Matsumoto Y.S., Tateno M., Iinuma Y., Matsumoto T, Toyohashi T., "Quoit Filter-a New Filter Based on Mathematical Morphology to Extract the Isolated Shadow, and Its Application to Automatic Detection of Lung Cancer in X-Ray CT", Proceedings of the 13th International Conference on Pattern Recognition, 1996, Vol. 2, pp. 3-7.

21. Mori, K. Hasegawa, J. Toriwaki, J. Anno, H. Katada, K., "Recognition of Bronchus in Three-Dimensional X-Ray CT Images with Applications to Virtualized Bronchoscopy System", Proceedings of the 13th International Conference on Pattern Recognition, 1996, Vol. 3, pp. 528- 532.

22. Li F., Sone S., Abe H., MacMahon H., Doi K., "Malignant versus Benign Nodules at CT Screening for Lung Cancer: Comparison of Thin Section CT Findings", Radiology, December 2004, pp. 793-798.